

Annual Review of Biomedical Engineering Point-of-Care Devices to Detect Zika and Other Emerging Viruses

Helena de Puig,^{1,2} Irene Bosch,³ James J. Collins,^{1,2,4,5}
and Lee Gehrke^{1,6}

¹Institute for Medical Engineering and Science, Massachusetts Institute of Technology, Cambridge, Massachusetts 02139, USA; email: hpuig@mit.edu, jmjc@mit.edu, lgehrke@mit.edu

²Wyss Institute for Biologically Inspired Engineering, Harvard University, Boston, Massachusetts 02115, USA

³E25Bio Inc., Cambridge, Massachusetts 02139, USA; email: ibosch@e25bio.com

⁴Department of Biological Engineering, Massachusetts Institute of Technology, Cambridge, Massachusetts 02139, USA

⁵Broad Institute of MIT and Harvard, Cambridge, Massachusetts 02142, USA

⁶Department of Microbiology, Harvard Medical School, Boston, Massachusetts 02115, USA

Annu. Rev. Biomed. Eng. 2020. 22:371–86

The *Annual Review of Biomedical Engineering* is
online at bioeng.annualreviews.org

<https://doi.org/10.1146/annurev-bioeng-060418-052240>

Copyright © 2020 by Annual Reviews.
All rights reserved

Keywords

rapid diagnostic test, virus, synthetic biology, lateral flow immunoassay, monoclonal antibody, synthetic genetic circuit, CRISPR/Cas, SHERLOCK

Abstract

Rapid diagnostic tests (point-of-care devices) are critical components of informed patient care and public health monitoring (surveillance applications). We propose that among the many rapid diagnostics platforms that have been tested or are in development, lateral flow immunoassays and synthetic biology-based diagnostics (including CRISPR-based diagnostics) represent the best overall options given their ease of use, scalability for manufacturing, sensitivity, and specificity. This review describes the identification of lateral flow immunoassay monoclonal antibody pairs that detect and distinguish between closely related pathogens and that are used in combination with functionalized multicolored nanoparticles and computational methods to deconvolute data. We also highlight the promise of synthetic biology-based diagnostic tests, which use synthetic genetic circuits that activate upon recognition of a pathogen-associated nucleic acid sequence, and discuss how the combined or parallel use of lateral flow immunoassays and synthetic biology tools may represent the future of scalable rapid diagnostics.

ANNUAL
REVIEWS **CONNECT**

www.annualreviews.org

- Download figures
- Navigate cited references
- Keyword search
- Explore related articles
- Share via email or social media

Contents

INTRODUCTION	372
LATERAL FLOW IMMUNOASSAYS FOR DETECTING AND DISTINGUISHING CLOSELY RELATED VIRUSES	373
NUCLEIC ACID- AND SYNTHETIC BIOLOGY-BASED DIAGNOSTIC TESTS	377
TECHNICAL CHALLENGES IN DEVELOPING POINT-OF-CARE DIAGNOSTICS FOR OUTBREAKS	382
Assessing Diagnostic Performance	382
Regional and Population Variations in the Performance of Diagnostic Tests	383
Specimen Collection	383
Incorporating Data from Rapid Diagnostic Tests into Medical Records and Shared Public Health Resources	383

INTRODUCTION

Human health monitoring as well as disease prevention and treatment are informed to great benefit by the accurate and timely detection and identification of pathogens. This is the domain of rapid diagnostic tests, which detect low concentrations of ligands to detect viral and bacterial pathogens and track markers that reflect human physiology, including pregnancy. As the name implies, a rapid diagnostic test is designed to report data quickly—that is, in under approximately 20 min. It can be used as a point-of-care (POC) instrument, to inform immediate patient care at the bedside, or as a surveillance device for epidemiology, when applied to routine monitoring for pathogen detection. In some examples, the basic design of rapid tests has remained relatively unchanged over decades; this is true, for example, for paper-fluidic lateral flow devices. In other cases, a new era of rapid diagnostics is emerging in the form of synthetic biology-based tests that can be activated by rehydration from a stable desiccated form to turn on genetic switches and amplification reactions to detect single-nucleotide sequence variations.

In this review, we first describe recent single and multiplexed paper-fluidic lateral flow immunoassay (LFIA) devices used to detect closely related viruses, focusing on combinatorial monoclonal antibody pairs that discriminate between closely related proteins. Included in this section is a description of computational methods that evaluate detection thresholds and calculate the area under the curve (AUC) to assign performance values. We note that LFIA technologies were reviewed recently by Banerjee & Jaiswal (1), and Wild (2) has edited an excellent handbook that not only emphasizes immunoassays but also describes terminology and definitions that are relevant to the development and performance of rapid diagnostic devices. We next discuss recent advances in synthetic biology approaches to developing rapid diagnostic devices. Unlike the LFIA, which was introduced in the 1980s (3), synthetic biology emerged only 20 years ago (4–7). Recent papers have summarized the contributions made by synthetic biology to diagnostic developments (8–10). This review focuses on the successes and challenges of developing and distributing synthetic biology devices for broad use. We note that lateral flow and synthetic biology approaches are distinct, but their complementary features may be the future of rapid diagnostics for detecting pathogens that threaten human health. We also describe in some detail the technical challenges that must be addressed when developing POC diagnostics for outbreaks.

LATERAL FLOW IMMUNOASSAYS FOR DETECTING AND DISTINGUISHING CLOSELY RELATED VIRUSES

Many human tropical viral infections present with similar symptoms—that is, fever, rash, headache, and malaise. In the absence of diagnostic tests, it is often difficult to distinguish among dengue fever, Zika disease, and chikungunya disease. Most infections are diagnosed as “fevers of unknown origin” because facilities, resources, or diagnostic devices are not available to detect and distinguish the pathogens (10). This problem is exacerbated by virus families that have different but related species (e.g., dengue viruses and Zika virus) that cause distinct pathologies despite their homologous viral proteins.

Our recent work has included a focus on developing and testing rapid diagnostics to detect and distinguish five viruses that share high homology: the four dengue virus serotypes and Zika virus (11). This was a challenging problem because the four dengue serotype NS1 (nonstructural 1) proteins share about 80% homology, meaning that antigenic determinants will be shared, thus complicating strategies to distinguish them by LFIA. Dengue and Zika NS1 proteins have greater than 50% homology, and although this is less similarity than among the dengue serotypes, crossover interference in dengue–Zika diagnostics is a significant problem (11). To initiate the process of developing an LFIA to detect and distinguish the four dengue serotypes, as well as Zika virus, we immunized mice with each of the NS1 proteins. The initial identification of antibodies for use in diagnostics is tedious and is most often accomplished by enzyme-linked immunosorbent assay (ELISA) in 96- or 384-well plates. However, the behavior of a monoclonal antibody in an ELISA is not necessarily predictive of its behavior in an LFIA; therefore, device developers recommend testing the selected antibodies in the LFIA format at the earliest opportunity in the development pipeline (2).

A matrix approach is used to test the binding characteristics of paired monoclonal antibodies by LFIA (**Figure 1**). The data in **Figure 1** demonstrate the differential binding properties of the monoclonal antibody (mAb) pairs. For example, mAb 243 showed preferential binding for dengue serotype 2 NS1 when combined with mAbs 323, 136, 243, 29, and 1, but little binding to Zika virus NS1. However, mAb 136 bound poorly to dengue serotype 4 NS1, but it bound to other dengue serotype NS1 and Zika virus NS1 in pairings with other mAbs. mAb 912 showed specificity for dengue serotype 1 NS1, while mAbs 29 and 900 cross-reacted with several dengue serotype NS1 proteins. These data demonstrate that although the NS1 proteins of dengue serotypes 1–4 and Zika viruses are homologous and elicit many cross-reactive antibody responses, it is possible to identify antibody pairs that distinguish the individual pathogens. These antibody pairs were used in an LFIA to test patients’ serum samples, and the resulting data, evaluated by receiver–operator curve (ROC) analysis, demonstrated excellent device performance (11).

In gold nanoparticle–based LFIA, a positive test signal is observed and detected as a red–purple band or dot that forms as the visible accumulation of gold nanoparticles. Gold nanoparticles are available in commercial kits for rapid and simple antibody conjugation; however, the cost is generally prohibitive for manufacturing scale-up. Alternatively, laboratory and commercial nanoparticle syntheses are relatively simple, can be performed with either gold or silver salts, and can yield a rainbow of nanoparticle colors (12–15). A consistent goal of using LFIA is to obtain the greatest amount of information from the smallest sample size in the shortest amount of time and with the greatest sensitivity, specificity, and limit of detection. Multiplexing—that is, detecting multiple pathogens with a single test—is an obvious approach but one that is often fraught with nonspecific binding interactions and cross-reactivity. However, the careful selection of antibody pairs—although time consuming and tedious—can generate rigorous multiplexed diagnostics. **Figure 2** shows the detection of three viral antigens in a multiplexed assay: dengue virus NS1

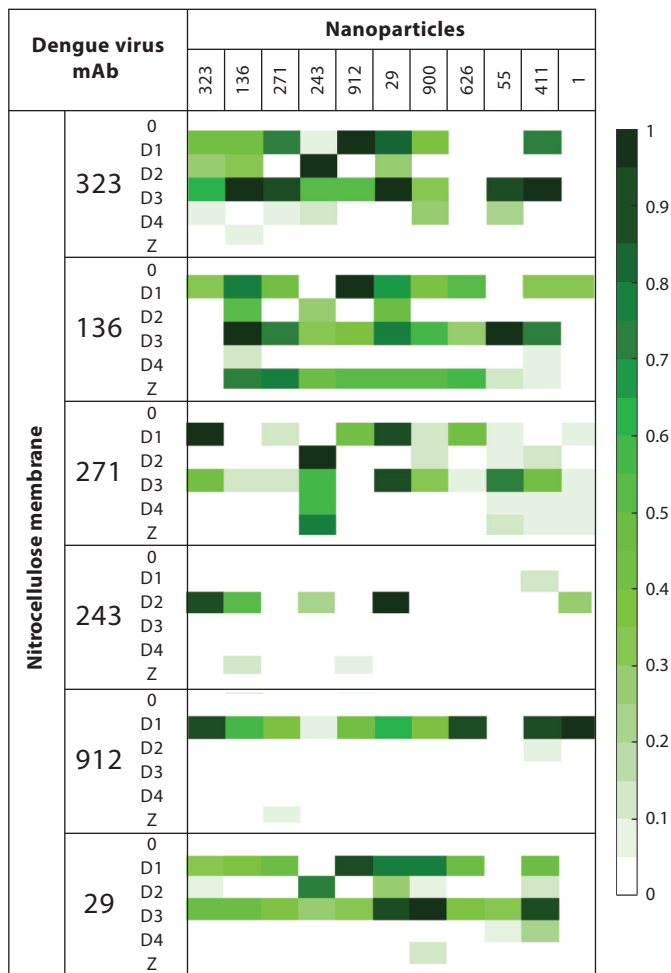


Figure 1

Matrix for testing monoclonal antibodies in pairs to detect and distinguish dengue and Zika NS1 proteins. The antibodies indicated by clone numbers on the y axis were immobilized on the LFIA membrane, while the antibodies on the x axis were conjugated to gold nanoparticles. Also shown for each antibody on the x axis are the dengue serotype NS1 antigens or the Zika NS1 protein antigens used with the dipstick. Every combination was tested, and dark green indicates the strongest binding signal, while white signifies no detectable binding at the LFIA test line. Figure adapted with permission from Reference 11. Abbreviations: 0, uninfected negative control; D1–4, dengue serotypes 1–4; LFIA, lateral flow immunoassay; mAb, monoclonal antibody; Z, Zika virus.

protein, chikungunya virus envelope protein, and Zika virus NS1 protein. These three viruses can co-circulate, and the acute symptoms of the infections are initially similar. The data in **Figure 2** demonstrate the functionality of a multiplexed test for dengue, Zika, and chikungunya viruses using a single-color gold nanoparticle. Although the single antigen tests show little cross-reactivity at the other test areas, a potential disadvantage of these tests is that it is difficult to determine whether there is cross-reactive binding if two positive signals appear, which suggests a co-infection. We next discuss the use of multicolored nanoparticles, which can be effective in evaluating cross-reactivity in multiplexed tests.

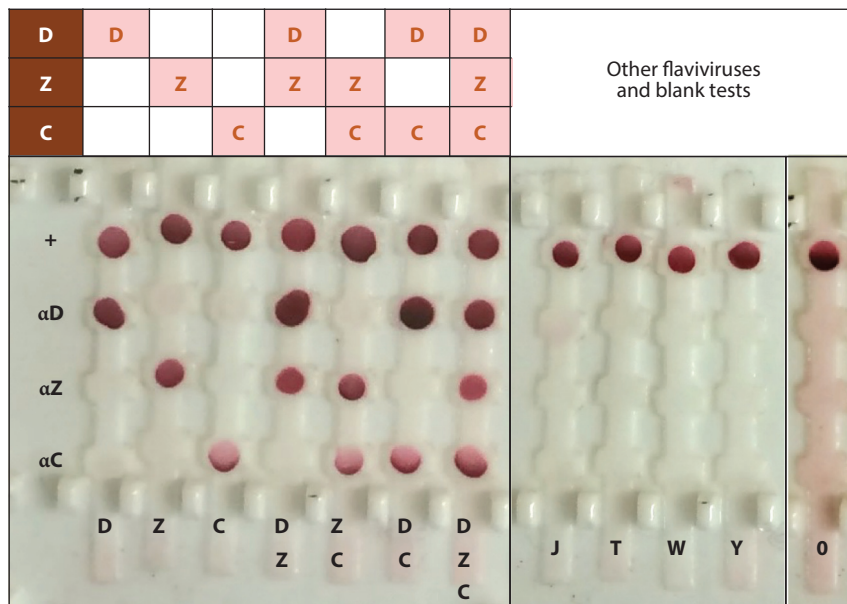


Figure 2

Multiplexed detection of dengue, Zika, and chikungunya viruses. The labels on the vertical axis denote rows of immobilized antibodies. Moving from left to right in the figure: First, the antigens are tested individually, which shows there is little cross-reactivity. Next, combinations of two sample antigens are tested, and little cross-reactivity is observed at the omitted antigen test area. Finally, all three antigens are combined.

Negative controls include NS1 proteins from related flaviviruses as well as uninfected negative controls. The labels on the horizontal axis refer to the antigen(s) present in the samples that were run. Abbreviations: 0, uninfected negative control; C, chikungunya envelope protein; D, dengue NS1 protein; DC, dengue NS1 and chikungunya envelope proteins; DZ, dengue and Zika virus NS1 proteins; DZC, dengue NS1, Zika NS1, and chikungunya envelope proteins; J, Japanese encephalitis virus NS1 protein; T, tick-borne encephalitis virus NS1 protein; αC, anti-chikungunya envelope protein; αD, anti-dengue NS1 protein; αZ, anti-Zika virus NS1 protein; W, West Nile virus NS1 protein; Y, yellow fever virus NS1 protein; Z, Zika virus NS1 and chikungunya envelope proteins.

The use of multicolored nanoparticles is advantageous in LFIA because it facilitates test multiplexing with the concurrent evaluation of cross-reactivity. Multicolored silver nanoparticles can be synthesized using a seed-mediated growth method (16). Yen et al. (15) demonstrated that Ebola, yellow fever, and dengue virus antigens could be detected using colored silver nanoparticles when the three assays were multiplexed into a single dipstick test (**Figure 3a,b**). Color adds a second specificity parameter to the tests—that is, color is present in addition to the test signal position on the strip. In control reactions, the identity of the immobilized antibody should match the identity of the corresponding antibody conjugated to the colored nanoparticle. The absence of a match, indicated by unexpected color, suggests nonspecific cross-reactive binding. With strong signals, the colors are easily distinguished; however, with weaker signals or in the case of cross-reactivity, the colors can be less discernible by eye.

Imaging and computational methods are used to quantify individual nanoparticle signals by RGB (red-green-blue) analysis in open source applications (such as ImageJ, developed by the US National Institutes of Health); further, principal component analysis (PCA) can be used to cluster the data for objective determination of test specificity (identifying true-positive signals) and sensitivity (identifying true-negative signals) (15) (**Figure 3**). At the completion of the dipstick run,

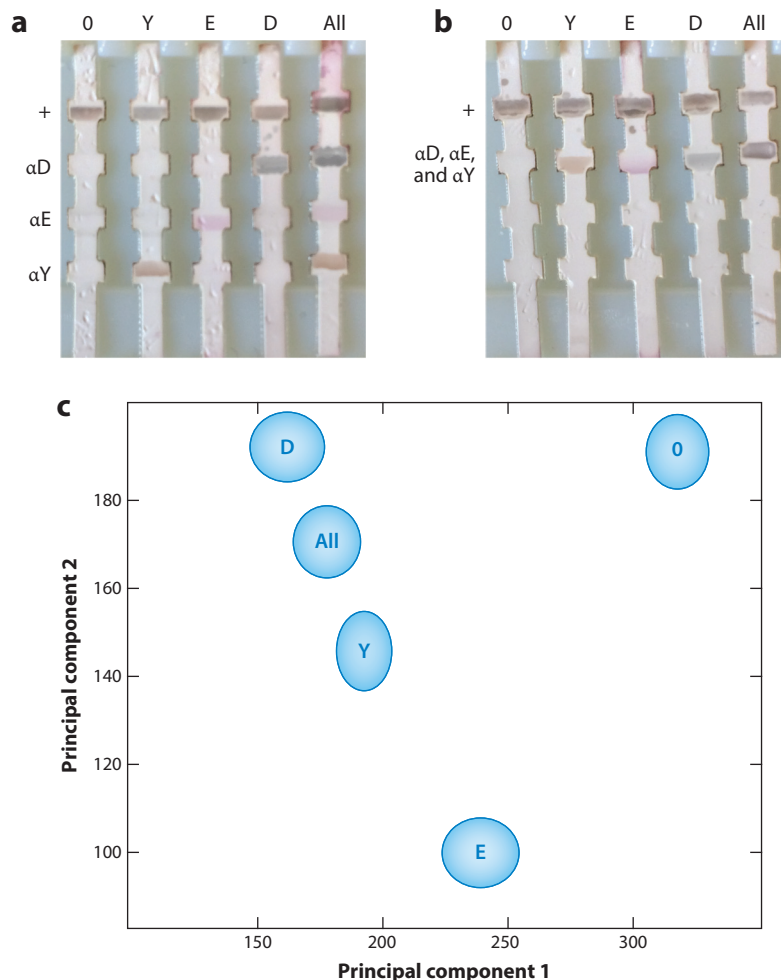


Figure 3

Multicolored silver nanoparticles can be used to detect and distinguish among Ebola virus glycoprotein, yellow fever virus NS1, and dengue virus NS1 proteins. (a) Antibodies against viral proteins are printed on individual detection areas in the nitrocellulose strips, and a mixture of disease-specific multicolored nanoparticles (NPs) flows through the strips. When each of the infectious diseases is present, the corresponding NPs form a colored band at the specific test line. (b) Disease-specific antibodies are then combined and printed into a single test line, which has different colors depending on the antigen present. (c) The RGB (red-green-blue) value of each antigen is calculated and followed by principal component analysis to discriminate the infectious diseases. The center of the ellipses and the length of their axes represent the mean and standard deviation, respectively. Figure adapted with permission from Reference 15. Abbreviations: +, anti-Fc positive control antibody; 0, uninfected negative control; D, dengue virus NS1 protein; E, Ebola virus glycoprotein; Y, yellow fever virus NS1 protein; αD, anti-dengue NS1 protein antibody; αE, anti-Ebola virus glycoprotein antibody; αY, anti-yellow fever virus NS1 protein antibody.

the strips are dried and photographed, often using a mobile phone camera. The resulting image is imported into image analysis software, such as ImageJ, for RGB color separation. These results are then imported into a MATLAB script that performs the PCA (Figure 3c). An important advantage of image analysis and PCA is that the data are objective, quantified, and expressed in a statistically

rigorous output. **Figure 3c** shows results demonstrating that each pair's signal is clearly separated from that of the other pairs; therefore, the detection is unequivocal. Cross-reactive binding is not observed in **Figure 3**, but if it were present, the resulting clusters would be shifted or unexpected clusters would appear. A potential disadvantage of image analysis and PCA is that post-run time is required to take the images and process the data. The image analysis could be standardized using test dipsticks for the development and validation of automated scripts. Through the use of a mobile phone camera to obtain images and process the data, a future POC device would be suitable to deliver a result and a diagnosis in only a few minutes.

NUCLEIC ACID- AND SYNTHETIC BIOLOGY-BASED DIAGNOSTIC TESTS

The interactions that regulate antibody-antigen binding, such as those used in LFIA and ELISAs, are complex and involve hydrogen bonds, hydrophobic interactions, and electrostatic and van der Waals forces (17). In contrast, nucleic acid recognition is straightforward and predictable. Base pairs of the four nucleic acid bases bind through Watson-Crick pairing: adenine (A) binds to thymine (T) [or uracil (U) in the case of RNA] through two hydrogen bonds, and guanine (G) binds to cytosine (C) through three hydrogen bonds. Due to the simplicity of DNA binding, it is possible to predict the binding thermodynamics, secondary structure, and hybridization of nucleic acid sequences *in silico*. Nucleic acid-based diagnostics capitalize on DNA or RNA base pair recognition.

The current gold standard of nucleic acid testing is polymerase chain reaction (PCR) (18, 19). PCR has high sensitivity and specificity; however, it is typically avoided in POC applications, as it is slow and its use requires a thermal cycler, fixed location, expensive materials, and trained personnel (20, 21). PCR is susceptible to contamination, and PCR inhibitors are present in human blood and body fluids; thus, careful sample preparation is essential (22). Moreover, PCR reagents (proteins and dyes) are sensitive to humidity, light, and temperature, and they require cold-chain transport.

Several DNA amplification techniques exist that obviate the use of a thermal cycler (23). Low temperature isothermal amplification technologies have been developed, extensively studied, and contrasted in literature reviews (20, 24–26). Isothermal amplification technologies include nucleic acid sequence-based amplification (NASBA) (27), helicase-dependent amplification, recombinase polymerase amplification (RPA), rolling circle amplification, and loop-mediated isothermal amplification. Frequent issues with isothermal amplification techniques involve off-target amplification, difficulty in multiplexing the assays, the need for purification and a fixed location, and the strict requirement for cold-chain transport of reagents.

New technologies based on synthetic biology allow for the detection of DNA and RNA sequences in a freeze-dried form that is stable for long-term storage at room temperature. Synthetic biology combines biological sciences with engineering principles to create new biomolecular functions for practical applications. In the context of POC diagnostics, synthetic biology efforts have been focused on building sensors (i.e., toehold switches) that are coupled to a measurable signal, such as the production of an output protein. These synthetic gene circuits arise from the engineered assembly of natural molecular components.

During the past few years, our lab has developed a platform for rapidly creating synthetic biology-based diagnostics that are inexpensive, portable, and easy to use (28, 29). The platform is a combination of two technologies: programmable molecular sensors called RNA toehold switches (**Figure 4a**) and *in vitro* freeze-dried cell-free expression systems. The toehold switch sensors can be rationally designed to bind and sense virtually any RNA sequence (30). The DNA encoding

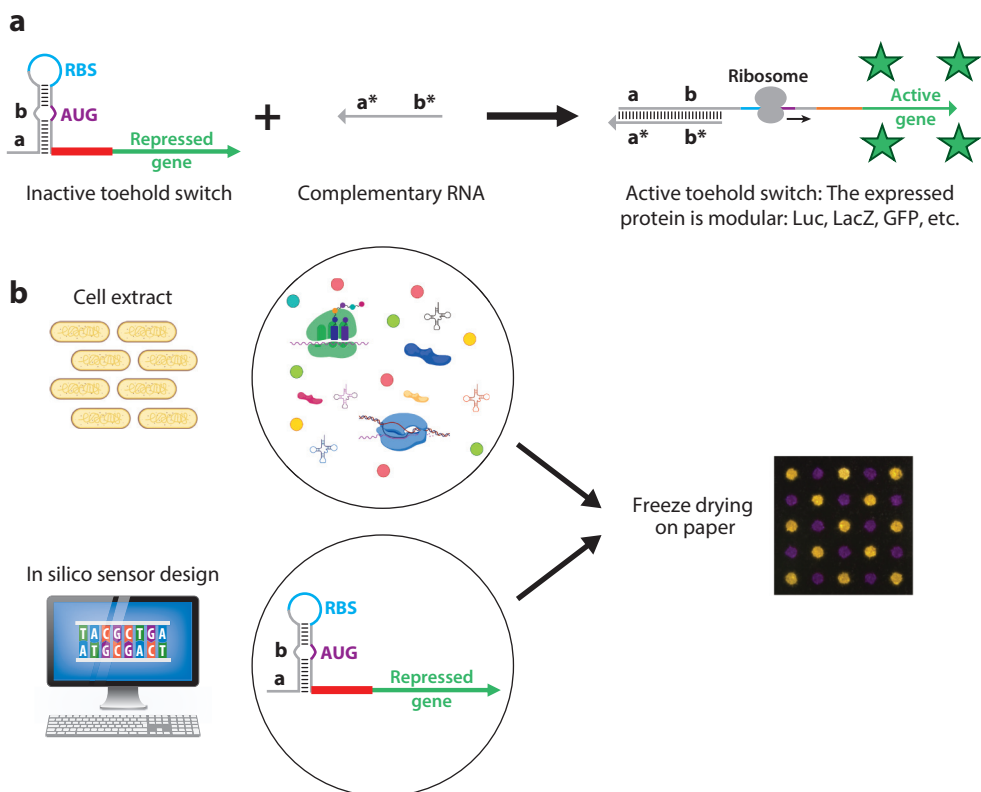


Figure 4

(a) Toehold riboregulator for RNA detection. The toehold switch RNA sensor is designed with a toehold region (a + b) that is complementary to the target trigger RNA (a* + b*). In the off state, translation is inhibited by sequestering the start codon (AUG) and ribosome binding site (RBS) in a hairpin loop. When target trigger RNA is present, it binds the corresponding toehold region on the switch RNA, opening the hairpin and enabling reporter gene translation. Active toehold switches are modular and can generate output proteins that produce fluorescence (e.g., green fluorescent protein, GFP), luminescence (luciferase, Luc), or a color change visible to the naked eye (LacZ, LacZ β -galactosidase). (b) Sequence information from online databases can be used to design toehold switch RNA sensors in silico. Sensors can be freeze-dried with cell-free transcription and translation extracts that can be deployed in the field as diagnostic tests; these are stable at room temperature for more than one year. Diagnostics can be activated upon rehydration. Color change visible to the naked eye can be observed through the expression of β -galactosidase. A color change from yellow to purple indicates that toehold switches were activated by the trigger. Figure adapted with permission from References 28 and 29.

the sensors can be lyophilized onto paper along with cell-free transcription and translation components (**Figure 4b**), and these materials have been shown to remain stable at room temperature for longer than 1 year. The system is activated by adding a sample containing the target RNA (29). This freeze-dried, paper-based, cell-free system allows for the implementation of toehold switch sensors in a sterile, abiotic manner that can be easily developed into a POC diagnostic. Because these cell-free systems perform in vitro, they do not face the complexities posed by cell-based synthetic biology approaches that import biomolecular components into the intracellular space, thus making them easily modifiable and excellent platforms for bioengineering.

Toehold switch sensors combined with freeze-dried cell-free expression systems have been used to create paper-based sensors to detect markers of antibiotic resistance (28), Ebola virus (28), and Zika virus (29), and to study the microbiome (31). Despite these proof-of-concept demonstrations, several challenges remain for the practical implementation of paper-based diagnostics, such as meeting the detection thresholds required for field use. To overcome this limitation, amplification strategies for target nucleic acids (i.e., PCR, NASBA, or RPA) have been combined with toehold switch detection (29, 31), yielding limits of detection within the range of interest for many clinical applications. The advantages of cell-free synthetic biology-based diagnostics over quantitative PCR are their cost and their ability to be used for multiplexed detection. RNA can be quantified in 3–5 h at a low temperature at a cost of between \$2.00 and \$16.00 per transcript (31). Moreover, in addition to fluorescence outputs, the sensors can be designed to produce luminescence as well as enzymes that generate color changes visible to the naked eye (29), which are interesting features for POC applications in low-resource settings lacking technical infrastructure.

A newer class of synthetic biology-based diagnostic devices emerged with the discovery of CRISPR-Cas systems. CRISPR-based diagnostics leverage the programmable RNA-guided endonucleases (Cas enzymes) of CRISPR-associated microbial adaptive immune systems. Cas enzymes have evolved to recognize specific target foreign nucleic acid sequences and to subsequently neutralize them through cleavage. Cas enzymes can be easily programmed to detect any nucleic acid sequence of interest by simply changing the sequence of the guide RNA. Due to their high specificity and enzymatic activity, CRISPR-Cas systems have led to the rapid development of a new class of diagnostics for infectious diseases.

CRISPR-Cas9 was the first protein of the CRISPR family used in diagnostic applications. CRISPR-Cas9 diagnostics typically use a Cas9 enzyme to cleave a nucleic acid sequence of interest, and they then use a different technology as a readout, such as toehold switches (29), sequencing (32), optical DNA maps (33), quantitative PCR (34–37), or electrochemistry (38, 39). Portable, freeze-dried diagnostics using CRISPR-Cas9 combine Cas9 with isothermal amplification techniques, i.e., NASBA and toehold switch sensors, to accurately distinguish between closely related virus strains (29). This technique is termed NASBA-CRISPR cleavage (NASBACC) and capitalizes on Cas9's ability to selectively cleave DNA only in the presence of a strain-specific protospacer adjacent motif. In NASBACC, viral RNA is amplified using a reverse primer that appends a synthetic trigger sequence, which can, in turn, activate a synthetic toehold switch sensor (**Figure 5a**). After Cas9 cleavage, the presence or absence of a strain-specific protospacer adjacent motif results in truncated or full-length DNA fragments, respectively. Truncated strands are unable to activate the toehold switch. In contrast, full-length strands that have not been cleaved by Cas9 activate the synthetic toehold switch. Toehold switch activation induces a yellow to purple color change on a paper disc, allowing for reliable strain differentiation. This approach enables the detection of single-nucleotide polymorphisms (**Figure 5b**). In different applications, catalytically dead Cas9 enzymes that do not induce DNA cleavage have also been used to capture specific DNA sequences, which is followed by detection by electrochemistry (38, 39) or fluorescence in situ hybridization (40).

These DNA-sensing technologies have tremendous diagnostic potential. However, they are inherently limited by the one-to-one stoichiometry of Cas9. Consequently, focus has been recently placed on developing approaches using Cas enzymes that exhibit multi-turnover kinetics and, thus, are able to provide signal amplification upon detection of the target nucleic acid sequence.

The discovery of the catalytic collateral nuclease activity induced by Cas12, Cas13, or Cas14 enzymes led to the rapid development of new nucleic acid diagnostics with improved sensitivities. The first of these platforms is known as SHERLOCK (for specific high-sensitivity enzymatic reporter unlocking), and it combines isothermal RPA or reverse transcription RPA with

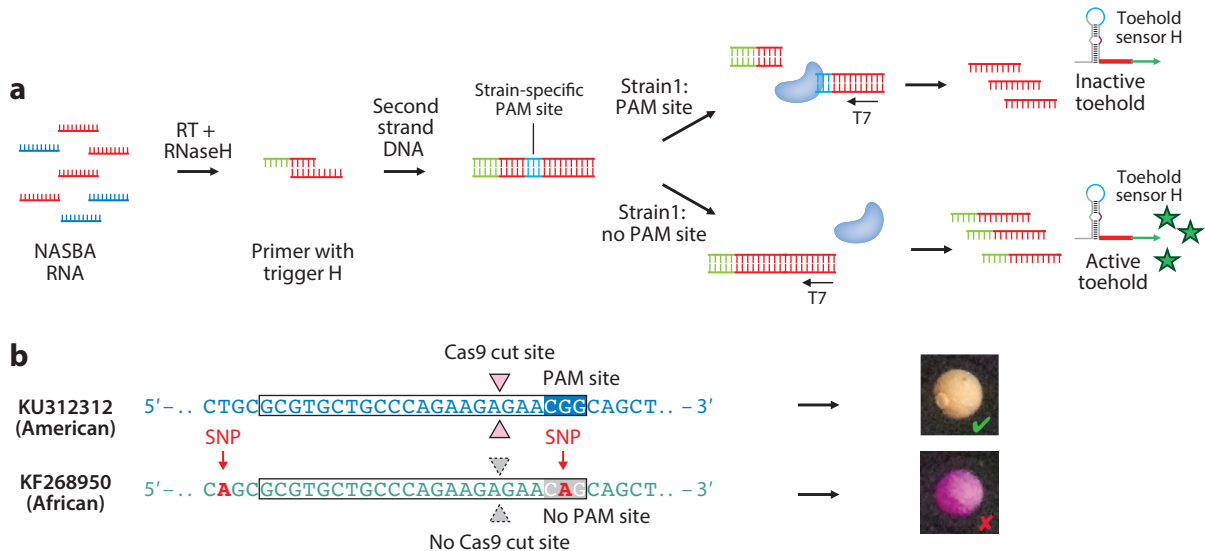


Figure 5

(a) Toehold Cas9 genotyping of single-nucleotide polymorphisms (SNPs) for Zika virus. A synthetic trigger sequence is attached to a nucleic acid sequence-based amplified (NASBA) RNA fragment through reverse transcription. Then, Cas9 cleaves double-stranded DNA sequences that contain a protospacer adjacent motif (PAM) site, leading to the production of full-length or truncated trigger RNA. Full-length trigger RNA contains the trigger H sequence, which activates a toehold switch sensor (sensor H). (b) A SNP between African (GenBank: KF268950) and American (GenBank: KU312312) Zika strains at site 7330 disrupts a PAM site. This allows for Cas9-mediated DNA cleavage only in the American strain, and no color change is observed from inactive toeholds. Figure adapted with permission from Reference 29.

Cas13a cleavage (41). The guide RNA–Cas13a complex activates after specific binding to the target RNA sequence. It then engages in collateral cleavage of nearby reporter RNA that is coupled to a quenched fluorophore, providing a fluorescent signal for pathogen detection (**Figure 6a**). The high specificity of this technique allows it to differentiate between closely related Zika and dengue viruses (**Figure 6b**) and also between different Zika virus strains (African and America Zika strains) (41). The sensors and enzymes can be stabilized by freeze drying, which facilitates sensor transport and storage. SHERLOCK version 2 (42) further introduces improvements that include single-reaction multiplexing with orthogonal CRISPR enzymes (**Figure 6c**), enhanced sensitivity, and enhanced portability by using paper-based lateral flow readouts (**Figure 6d**). Single-reaction multiplexing of several targets can be achieved by combining multiple Cas13 and Cas12 nucleases with orthogonal reporters conjugated to different fluorophores, which provide target-specific detection at different wavelengths. In addition, coupling the assays to paper-based lateral flow readouts increases the portability of the assays for POC applications in low-resource settings (**Figure 6d**). Key challenges in the development of POC nucleic acid diagnostics are the presence of reaction inhibitors in the sample matrix (e.g., blood, saliva, urine) and the requirement to lyse pathogens in order to access target nucleic acids. To overcome these limitations, SHERLOCK was recently combined with HUDSON (heating unextracted diagnostic samples to obliterate nucleases) (43), thus enabling pathogens to be detected directly from body fluids. HUDSON uses heat and chemical reduction to inactivate nucleases present in body fluids and to lyse viral particles, which releases target nucleic acids into solution. Combining HUDSON with SHERLOCK allows for highly sensitive detection of dengue virus within 2 h in samples of whole blood, serum, and saliva.

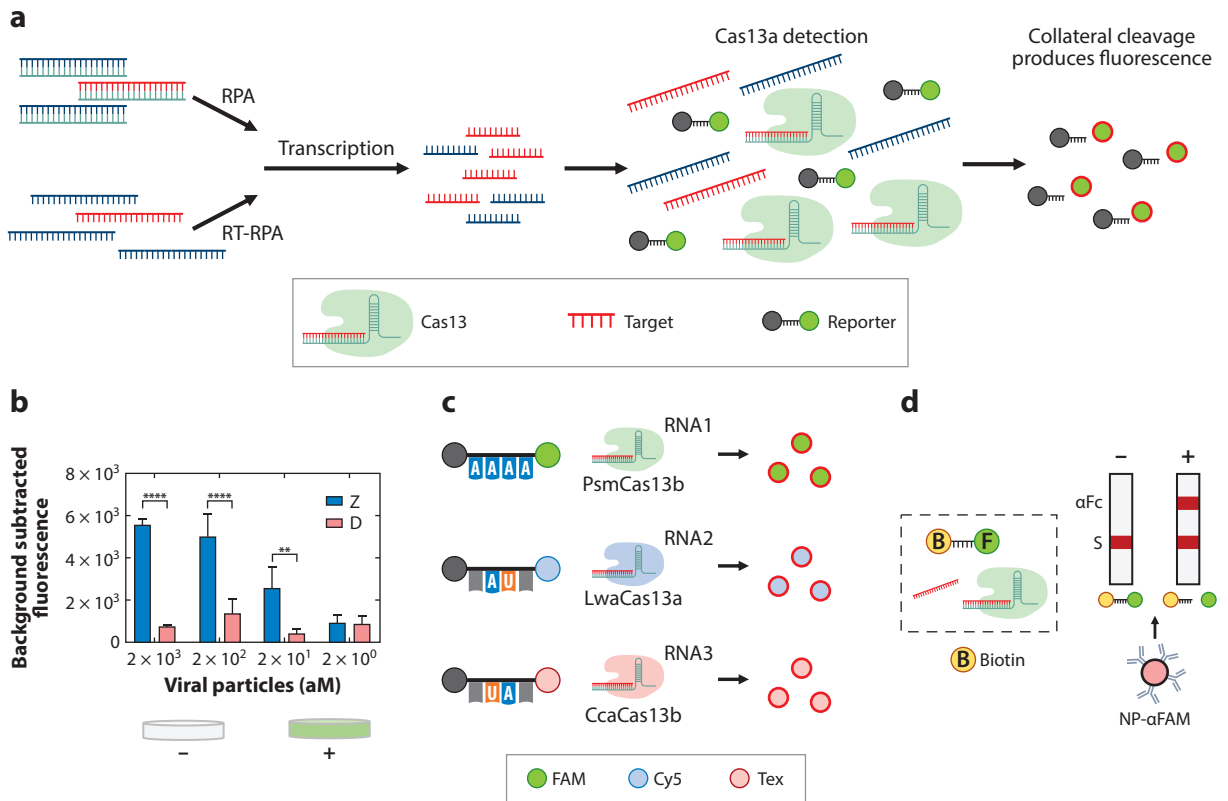


Figure 6

(a) The SHERLOCK (specific high-sensitivity enzymatic reporter unlocking) platform. Trigger double-stranded DNA or RNA can be amplified by, respectively, isothermal recombinase polymerase amplification (RPA) or reverse transcription RPA (RT-RPA). T7 polymerase is then used to transcribe trigger RNA for the Cas13 reaction. Upon activation, Cas13a engages in the collateral cleavage of labeled nontarget RNA, leading to an increase in fluorescence. (b) Cas13a can be freeze-dried on paper and used for sensitive and specific detection of low (attomolar; aM) concentrations of Zika virus (Z), without cross-reacting with dengue virus (D). (c) Multiplexed SHERLOCK capitalizes on the differential collateral activities of Cas13a and Cas13b orthologs. PsmCas13b, LwaCas13a, and CcaCas13b have preferential collateral activities on specific orthogonal dinucleotide bases. Therefore, attaching each specific dinucleotide reporter to different quenched fluorophores, i.e., FAM, Cy5, and Tex, allows for simultaneous detection of several RNA targets. (d) Lateral flow detection with SHERLOCK. A reporter single-stranded RNA molecule contains both biotin (B) and FAM (F) moieties. In the presence of the trigger sequence (+), Cas13a cleaves the single-stranded RNA reporter, and nanoparticles (NPs) coated with an anti-FAM (α FAM) antibody reach the anti-Fc band, leading to an observable signal in both the streptavidin (S) band and the anti-Fc (α Fc) band. In contrast, when the trigger sequence is not present (-), NPs accumulate in the S band and no signal is observed in the α Fc band. Figure adapted with permission from References 41 and 42.

Similar techniques, DETECTR (DNA endonuclease-targeted CRISPR *trans* reporter) and HOLMES (one-Hour Low-cost Multipurpose highly Efficient System), combine isothermal RPA with Cas12a (44, 45) or Cas14a (46) enzymatic activities. In DETECTR, CRISPR guide RNA-Cas12a complexes activate after binding to target single-stranded DNA or dsDNA. Active Cas12a engages in indiscriminate cleavage of single-stranded DNA that is coupled to a fluorescent reporter. DETECTR has been used to distinguish between human papillomavirus 16 (HPV16) and HPV18 in clinical samples (44), and the results agree with those of an approved PCR-based assay. Overall, CRISPR-Cas-based diagnostics combine the high specificity of CRISPR-Cas systems with isothermal amplification technologies to provide rapid diagnostic tests at the point of care

that can reach detection limits comparable to those of quantitative PCR at a fraction of the cost and in a form that can be used in the field.

CRISPR-based diagnostics hold great promise for POC applications due to their sensitivity, specificity, multiplexing capacity, ease of use, low cost, and capacity to detect virtually any nucleic acid sequence. However, they are relatively new and have not been tested beyond proof-of-concept applications, making it difficult to estimate their potential impact on POC diagnostics. CRISPR-based diagnostics can be compared with other nucleic acid detection methods, such as PCR. In contrast with PCR, SHERLOCK and DETECTR combine an isothermal amplification step with a detection step that further amplifies the signal and also provides increased specificity based on CRISPR guide RNA target recognition. In addition, CRISPR-based assays can be freeze-dried and easily deployed, because they operate at low temperatures and do not require a thermal cycler. While some isothermal amplification technologies, such as RPA, can also be run under similar conditions, they often suffer from low specificity due to low-temperature primer annealing. In contrast, CRISPR effectors have evolved to achieve specific recognition of nucleic acids at physiological temperatures, thus widening their application in POC diagnostics.

TECHNICAL CHALLENGES IN DEVELOPING POINT-OF-CARE DIAGNOSTICS FOR OUTBREAKS

Assessing Diagnostic Performance

Assessing diagnostic accuracy is important in evaluating the performance of POC diagnostic tests. In order to make a decision about whether to promote the clinical use of a new assay, evidence is required that using the new test either increases accuracy over previous assays or has the equivalent accuracy but offers additional advantages (47). Diagnostic accuracy refers to the ability of the test to distinguish between the absence or presence of disease. Accuracy can be quantified by measures such as sensitivity, specificity, predictive values, or ROCs.

A perfect diagnostic test should completely discriminate between infected and uninfected people. For binary tests that distinguish between the presence or absence of disease, the cutoff parameter is used to divide results into categories in which values above the cutoff are scored positive for the presence of disease and values below the cutoff indicate the absence of disease. However, a perfect diagnostic test that can completely differentiate infected people from uninfected people does not exist. Sometimes people without disease may have results above the cutoff (false positive; FP) and people with disease may have values below the cutoff (false negative; FN). Therefore, the cutoff divides the population into four subgroups:

- true positive (TP)—patients with the disease who have results above the cutoff,
- false positive (FP)—patients without the disease who have results above the cutoff,
- true negative (TN)—patients without the disease who have results below the cutoff,
- false negative (FN)—patients with the disease who have results below the cutoff.

To calculate the sensitivity, specificity, and predictive values, a typical approach is to make a 2×2 table (**Supplemental Figure 1a**) that relates the gold standard (reference method) values to the readout of the new test. Sensitivity relates to a test's potential to recognize people with a disease, and it is defined as the probability of obtaining a positive test result in people with confirmed infections. Specificity is defined as the probability of obtaining a negative test result in people confirmed to be uninfected, and it expresses the test's potential to recognize patients who do not have a disease. The positive predictive value (PPV) indicates the probability that someone with a positive test result actually has the disease, and the negative predictive value (NPV) describes the probability that someone with a negative test result does not have the disease. Sensitivity and

specificity are not influenced by the prevalence of a disease in the population. In contrast, the PPV and NPV are influenced by the prevalence in the examined population. Therefore, the NPV and PPV from one study cannot be transferred to settings with a different population prevalence.

ROCs (**Supplemental Figure 1b**) show how sensitivity and specificity change with varying thresholds across all possible values. ROC graphs plot sensitivity (the TP rate) against $1 - \text{specificity}$ (the FP rate). The ROC goes from the point where the values for sensitivity and $1 - \text{specificity}$ are both 1 (top right corner) to the point where sensitivity and $1 - \text{specificity}$ are both 0 (bottom left corner). The shape of an ROC and its AUC can be used to estimate the discriminative power of a diagnostic test. The AUC of an ROC can have any value between 0 and 1. ROCs that have higher AUC are closer to the upper left corner of the graph (that is, where sensitivity and specificity are both high) and are better at discriminating between infected and uninfected people. A perfect diagnostic test has an AUC of 1, while a nondiscriminating test has an AUC of 0.5.

The measures of diagnostic accuracy are standardized, and excellent resources can be found in both the Cochrane Collaboration (<https://methods.cochrane.org/sdt>) and the Standards for Reporting of Diagnostic Accuracy (known as STARD) (<https://www.equator-network.org/reporting-guidelines/stard/>) guidelines. However, results assessing diagnostic accuracy are extremely sensitive to a study's design. For example, small sample sizes, differences in study populations, or differences in study methods can lead to inaccurate results. Moreover, in POC applications, physical constraints, such as limited water, temperature variations, unreliable power sources, or reagent stability during storage or transportation, can also have large impacts on the performance of a diagnostic test.

Regional and Population Variations in the Performance of Diagnostic Tests

Many factors influence the performance of POC diagnostic tests, such as the prevalence of disease, the age of the patient, the acquisition of partial immunity, and co-infection with other diseases. Therefore, diagnostic tests need to be evaluated in a clinically relevant population. The term commonly used to describe this heterogeneity is spectrum bias, and it occurs when the performance of a diagnostic test varies across subgroups of patients and not all of those subgroups are adequately represented in a study of that test's performance. Sources of spectrum bias include differences in demographic features within the population, disease severity, disease prevalence, and a distorted selection of participants used for analysis. Therefore, when developing POC diagnostics, it is important to validate the assays in the settings and populations in which they will be used.

Specimen Collection

Sample collection and processing are critical steps in diagnosis. However, the manually intensive activities of sample collection and processing are some of the most error-prone steps in diagnosis. Collecting the wrong sample type, for example, can reduce the accuracy of a diagnostic test (48). Sample collection technologies that are used in high-resource settings might not be available for POC applications used during outbreaks. Thus, ideally, POC assays would be packaged and tested with a paired specimen collection device for each application to ensure lower variability of results.

Incorporating Data from Rapid Diagnostic Tests into Medical Records and Shared Public Health Resources

Rapid diagnostic tests can inform clinical care decisions and also provide surveillance data for epidemiological studies. Important challenges for future work in the field of rapid diagnosis will be

to define how data from rapid diagnostic tests are incorporated into a patient's permanent medical record and how the global community will define standards for collecting, storing, accessing, and protecting patients' data. Although the use of electronic medical records is expanding, results from virus diagnostics are generally not part of the interoperability requirements for Health Level Seven (known as HL7) medical records. Today, there are only a few examples of standardized reporting platforms for the results of rapid tests for infectious diseases that have been used successfully in multiple countries (49).

SUMMARY POINTS

1. Lateral flow immunoassays and synthetic biology-based diagnostic tests are widely separated on the technology spectrum, but they offer complementary approaches for detecting and diagnosing disease, and these approaches may benefit patients.
2. Lateral flow immunoassays are relatively inexpensive rapid tests that can be multiplexed, developed using multicolored nanoparticles, and analyzed using imaging software and straightforward computational methods (such as principal component analysis) to yield clear test results.
3. Synthetic biology-based diagnostics can detect low concentrations of target nucleic acids in relevant sample matrices. Toehold switch sensors, as well as CRISPR-Cas-based diagnostics, can be used for low-cost, sensitive, and specific pathogen detection.

FUTURE ISSUES

1. How will the diagnostics community incorporate data from rapid diagnostic tests into medical records and shared public health resources? Currently, virus diagnostic results are generally not part of the Health Level 7 standards for interoperable medical records.
2. How can the culture of the diagnostic testing industry be changed from being reactive (i.e., generating diagnostics after an outbreak has occurred) to proactive (i.e., preparing reagents for pathogen diagnostics in advance of outbreaks)?

DISCLOSURE STATEMENT

I.B. and L.G. are cofounders of E25Bio. J.J.C. is a cofounder and director of Sherlock Biosciences. L.G. holds patents on flavivirus monoclonal antibodies and design of rapid diagnostics.

ACKNOWLEDGMENTS

We are grateful to our many collaborators around the world who have generously provided samples and thoughtful critiques during the course of this work, and we apologize to all of the investigators whose valuable research was not cited in this text because of limited space.

LITERATURE CITED

1. Banerjee R, Jaiswal A. 2018. Recent advances in nanoparticle-based lateral flow immunoassay as a point-of-care diagnostic tool for infectious agents and diseases. *Analyst* 143:1970–96

2. Wild D, ed. 2013. *The Immunoassay Handbook: Theory and Applications of Ligand Binding, ELISA and Related Techniques*. Oxford: Elsevier. 4th ed.
3. Leuvering JH, Thal PJ, van der Waart M, Schuurs AH. 1980. Sol particle immunoassay (SPIA). *J. Immunoass.* 1:77–91
4. Isaacs FJ, Dwyer DJ, Ding CM, Pervouchine DD, Cantor CR, Collins JJ. 2004. Engineered riboregulators enable post-transcriptional control of gene expression. *Nat. Biotechnol.* 22:841–47
5. Cameron DE, Bashor CJ, Collins JJ. 2014. A brief history of synthetic biology. *Nat. Rev. Microbiol.* 12:381–90
6. Elowitz MB, Leibler S. 2000. A synthetic oscillatory network of transcriptional regulators. *Nature* 403:335–38
7. Gardner TS, Cantor CR, Collins JJ. 2000. Construction of a genetic toggle switch in *Escherichia coli*. *Nature* 403:339–42
8. Slomovic S, Pardee K, Collins JJ. 2015. Synthetic biology devices for in vitro and in vivo diagnostics. *PNAS* 112:14429–35
9. Glushakova LG, Alto BW, Kim MS, Hutter D, Bradley A, et al. 2019. Multiplexed kit based on Luminex technology and achievements in synthetic biology discriminates Zika, chikungunya, and dengue viruses in mosquitoes. *BMC Infect. Dis.* 19:418
10. McGregor AC, Moore DA. 2015. Infectious causes of fever of unknown origin. *Clin. Med.* 15:285–87
11. Bosch I, de Puig H, Hiley M, Carre-Camps M, Perdomo-Celis F, et al. 2017. Rapid antigen tests for dengue virus serotypes and Zika virus in patient serum. *Sci. Transl. Med.* 9:eaan1589
12. de Puig H, Federici S, Baxamusa SH, Bergese P, Hamad-Schifferli K. 2011. Quantifying the nanomachinery of the nanoparticle–biomolecule interface. *Small* 7:2477–84
13. de Puig H, Tam JO, Yen C-W, Gehrke L, Hamad-Schifferli K. 2015. The extinction coefficient of gold nanostars. *J. Phys. Chem. C* 119:17408–15
14. Tam JO, de Puig H, Yen C-W, Bosch I, Gómez-Márquez J, et al. 2016. A comparison of nanoparticle–antibody conjugation strategies in sandwich immunoassays. *J. Immunoass. Immunochem.* 38:355–77
15. Yen C-W, de Puig H, Tam JO, Gómez-Márquez J, Bosch I, et al. 2015. Multicolored silver nanoparticles for multiplexed disease diagnostics: distinguishing dengue, yellow fever, and Ebola viruses. *Lab Chip* 15:1638–41
16. Homan KA, Souza M, Truby R, Luke GP, Green C, et al. 2012. Silver nanoplate contrast agents for in vivo molecular photoacoustic imaging. *ACS Nano* 6:641–50
17. de Puig H, Bosch I, Gehrke L, Hamad-Schifferli K. 2017. Challenges of the nano–bio interface in lateral flow and dipstick immunoassays. *Trends Biotechnol.* 35:1169–80
18. Mullis K, Faloona F, Scharf S, Saiki R, Horn G, Erlich H. 1986. Specific enzymatic amplification of DNA in vitro: the polymerase chain reaction. *Cold Spring Harb. Symp. Quant. Biol.* 51:263–73
19. Saiki RK, Scharf S, Faloona F, Mullis KB, Horn GT, et al. 1985. Enzymatic amplification of beta-globin genomic sequences and restriction site analysis for diagnosis of sickle cell anemia. *Science* 230:1350–54
20. Zarei M. 2017. Advances in point-of-care technologies for molecular diagnostics. *Biosens. Bioelectron.* 98:494–506
21. Loonen AJ, Schuurman R, van den Brule AJ. 2012. Highlights from the 7th European Meeting on Molecular Diagnostics. *Expert Rev. Mol. Diagn.* 12:17–19
22. Bar T, Kubista M, Tichopad A. 2012. Validation of kinetics similarity in qPCR. *Nucleic Acids Res.* 40:1395–406
23. Roper MG, Easley CJ, Landers JP. 2005. Advances in polymerase chain reaction on microfluidic chips. *Anal. Chem.* 77:3887–93
24. Mayboroda O, Katakis I, O’Sullivan CK. 2018. Multiplexed isothermal nucleic acid amplification. *Anal. Biochem.* 545:20–30
25. Li J, Macdonald J. 2015. Advances in isothermal amplification: novel strategies inspired by biological processes. *Biosens. Bioelectron.* 64:196–211
26. Giuffrida MC, Spoto G. 2017. Integration of isothermal amplification methods in microfluidic devices: recent advances. *Biosens. Bioelectron.* 90:174–86

27. Deiman B, van Aarle P, Sillekens P. 2002. Characteristics and applications of nucleic acid sequence-based amplification (NASBA). *Mol. Biotechnol.* 20:163–79
28. Pardee K, Green AA, Ferrante T, Cameron DE, DaleyKeyser A, et al. 2014. Paper-based synthetic gene networks. *Cell* 159:940–54
29. Pardee K, Green AA, Takahashi MK, Braff D, Lambert G, et al. 2016. Rapid, low-cost detection of Zika virus using programmable biomolecular components. *Cell* 165:1255–66
30. Green AA, Silver PA, Collins JJ, Yin P. 2014. Toehold switches: de-novo-designed regulators of gene expression. *Cell* 159:925–39
31. Takahashi MK, Tan X, Dy AJ, Braff D, Akana RT, et al. 2018. A low-cost paper-based synthetic biology platform for analyzing gut microbiota and host biomarkers. *Nat. Commun.* 9:3347
32. Gu W, Crawford ED, O'Donovan BD, Wilson MR, Chow ED, et al. 2016. Depletion of Abundant Sequences by Hybridization (DASH): using Cas9 to remove unwanted high-abundance species in sequencing libraries and molecular counting applications. *Genome Biol.* 17:41
33. Muller V, Rajer F, Frykholm K, Nyberg LK, Quaderi S, et al. 2016. Direct identification of antibiotic resistance genes on single plasmid molecules using CRISPR/Cas9 in combination with optical DNA mapping. *Sci. Rep.* 6:37938
34. Zhang BB, Wang Q, Xu XH, Xia Q, Long FF, et al. 2018. Detection of target DNA with a novel Cas9/sgRNAs-associated reverse PCR (CARP) technique. *Anal. Bioanal. Chem.* 410:2889–900
35. Lee SH, Yu J, Hwang GH, Kim S, Kim HS, et al. 2017. CUT-PCR: CRISPR-mediated, ultrasensitive detection of target DNA using PCR. *Oncogene* 36:6823–29
36. Zhang BB, Xia Q, Wang Q, Xia XY, Wang JK. 2018. Detecting and typing target DNA with a novel CRISPR-typing PCR (ctPCR) technique. *Anal. Biochem.* 561:37–46
37. Wang Q, Zhang BB, Xu XH, Long FF, Wang JK. 2018. CRISPR-typing PCR (ctPCR), a new Cas9-based DNA detection method. *Sci. Rep.* 8:14126
38. Koo B, Kim DE, Kweon J, Jin CE, Kim SH, et al. 2018. CRISPR/dCas9-mediated biosensor for detection of tick-borne diseases. *Sens. Actuators B* 273:316–21
39. Hajian R, Balderston S, Tran T, deBoer T, Etienne J, et al. 2019. Detection of unamplified target genes via CRISPR–Cas9 immobilized on a graphene field-effect transistor. *Nat. Biomed. Eng.* 3:427–37
40. Guk K, Keem JO, Hwang SG, Kim H, Kang T, et al. 2017. A facile, rapid and sensitive detection of MRSA using a CRISPR-mediated DNA FISH method, antibody-like dCas9/sgRNA complex. *Biosens. Bioelectron.* 95:67–71
41. Gootenberg JS, Abudayyeh OO, Lee JW, Essletzbichler P, Dy AJ, et al. 2017. Nucleic acid detection with CRISPR-Cas13a/C2c2. *Science* 356:438–42
42. Gootenberg JS, Abudayyeh OO, Kellner MJ, Joung J, Collins JJ, Zhang F. 2018. Multiplexed and portable nucleic acid detection platform with Cas13, Cas12a, and Csm6. *Science* 360:439–44
43. Myhrvold C, Freije CA, Gootenberg JS, Abudayyeh OO, Metsky HC, et al. 2018. Field-deployable viral diagnostics using CRISPR-Cas13. *Science* 360:444–48
44. Chen JS, Ma EB, Harrington LB, Da Costa M, Tian XR, et al. 2018. CRISPR-Cas12a target binding unleashes indiscriminate single-stranded DNase activity. *Science* 360:436–39
45. Li SY, Cheng QX, Wang JM, Li XY, Zhang ZL, et al. 2018. CRISPR-Cas12a-assisted nucleic acid detection. *Cell Discov.* 4:20
46. Harrington LB, Burstein D, Chen JS, Paez-Espino D, Ma E, et al. 2018. Programmed DNA destruction by miniature CRISPR-Cas14 enzymes. *Science* 362:839–42
47. Bossuyt PMM, Reitsma JB, Linnet K, Moons KGM. 2012. Beyond diagnostic accuracy: the clinical utility of diagnostic tests. *Clin. Chem.* 58:1636–43
48. De Paoli P. 2005. Biobanking in microbiology: from sample collection to epidemiology, diagnosis and research. *FEMS Microbiol. Rev.* 29:897–910
49. Dehnavieh R, Haghdoost A, Khosravi A, Hoseinabadi F, Rahimi H, et al. 2019. The District Health Information System (DHIS2): a literature review and meta-synthesis of its strengths and operational challenges based on the experiences of 11 countries. *Health Inf. Manag. J.* 48:62–75



Contents

Layer-by-Layer Biomaterials for Drug Delivery <i>Dablia Alkekhia, Paula T. Hammond, and Anita Shukla</i>	1
Swine Disease Models for Optimal Vascular Engineering <i>Michael Sturek, Moubamad Alloosh, and Frank W. Sellke</i>	25
The New Age of Cell-Free Biology <i>Vincent Noireaux and Allen P. Liu</i>	51
Transgenic and Diet-Enhanced Silk Production for Reinforced Biomaterials: A Metamaterial Perspective <i>Jung Woo Leem, Malcolm J. Fraser, and Young L. Kim</i>	79
4D Flow with MRI <i>Gilles Soulat, Patrick McCarthy, and Michael Markl</i>	103
Sparse Data-Driven Learning for Effective and Efficient Biomedical Image Segmentation <i>John A. Onofrey, Lawrence H. Staib, Xiaojie Huang, Fan Zhang, Xenophon Papademetris, Dimitris Metaxas, Daniel Rueckert, and James S. Duncan</i>	127
Three-Dimensional Single-Molecule Localization Microscopy in Whole-Cell and Tissue Specimens <i>Sheng Liu, Hyun Hub, Sang-Hyuk Lee, and Fang Huang</i>	155
Physiological Modeling and Simulation—Validation, Credibility, and Application <i>W. Andrew Pruett, John S. Clemmer, and Robert L. Hester</i>	185
Engineering Approaches for Addressing Opioid Use Disorder in the Community <i>Paul M. Griffin</i>	207
Hemodynamics of Cerebral Aneurysms: Connecting Medical Imaging and Biomechanical Analysis <i>Vitaliy L. Rayz and Aaron A. Cohen-Gadol</i>	231

Micromechanobiology: Focusing on the Cardiac Cell–Substrate Interface <i>Erica A. Castillo, Kerry V. Lane, and Beth L. Pruitt</i>	257
Computer-Aided Design of Microfluidic Circuits <i>Elishai Ezra Tsur</i>	285
Integrated Biophysical Modeling and Image Analysis: Application to Neuro-Oncology <i>Andreas Mang, Spyridon Bakas, Shashank Subramanian, Christos Davatzikos, and George Biros</i>	309
Elastin-Like Polypeptides for Biomedical Applications <i>Anastasia K. Varanko, Jonathan C. Su, and Asbutosh Chilkoti</i>	343
Point-of-Care Devices to Detect Zika and Other Emerging Viruses <i>Helena de Puig, Irene Bosch, James J. Collins, and Lee Gebrke</i>	371
Mitigating the Consequences of Subconcussive Head Injuries <i>Eric A. Nauman, Thomas M. Talavage, and Paul S. Auerbach</i>	387

Errata

An online log of corrections to *Annual Review of Biomedical Engineering* articles may be found at <http://www.annualreviews.org/errata/bioeng>